

Alterations in the photoactivation pathway of rhodopsin mutants associated with retinitis pigmentosa

Laia Bosch-Presegué^{1,*}, Eva Ramon¹, Darwin Toledo¹, Arnau Cordomí² and Pere Garriga¹

¹ Departament d'Enginyeria Química, Centre de Biotecnologia Molecular, Universitat Politècnica de Catalunya, Terrassa, Spain

² Laboratori de Medicina Computacional, Unitat de Bioestadística, Facultat de Medicina, Universitat Autònoma de Barcelona, Cerdanyola del Vallès, Spain

Keywords

altered equilibrium; metarhodopsin II; photointermediate stability; retinal degeneration; visual diseases

Correspondence

P. Garriga, Departament d'Enginyeria Química, Universitat Politècnica de Catalunya, 08222 Terrassa, Catalonia, Spain
Fax: +34 937398225
Tel: +34 937398568
E-mail: pere.garriga@upc.edu

*Present address

Chromatin Biology Laboratory, Cancer Epigenetics and Biology Program (PEBC), IDIBELL, Barcelona, Catalonia, Spain

(Received 23 November 2010, revised 1 February 2011, accepted 23 February 2011)

doi:10.1111/j.1742-4658.2011.08066.x

The visual photoreceptor rhodopsin undergoes a series of conformational changes upon light activation, eventually leading to the active metarhodopsin II conformation, which is able to bind and activate the G-protein, transducin. We have previously shown that mutant rhodopsins G51V and G89D, associated with retinitis pigmentosa, present photobleaching patterns characterized by the formation of altered photointermediates whose nature remained obscure. Our current detailed UV-visible spectroscopic analysis, together with functional characterization, indicate that these mutations influence the relative stability of the different metarhodopsin photointermediates by altering their equilibria and maintaining the receptor in a nonfunctional light-induced conformation that may be toxic to photoreceptor cells. We propose that G51V and G89D shift the equilibrium from metarhodopsin I towards an intermediate, recently named as metarhodopsin Ib, proposed to interact with transducin without activating it. This may be one of the causes contributing to the molecular mechanisms underlying cell death associated with some retinitis pigmentosa mutations.

Introduction

Rhodopsin is the visual photoreceptor responsible for dim light vision [1,2]. This receptor is located in the rod cell of the retina. It has seven transmembrane (TM) helices and is a prototypical member of the G-protein coupled receptors (GPCRs) superfamily [3–5]. Rhodopsin was the first member of this superfamily for which a high-resolution structure became available by X-ray crystallography [6]. For almost a decade, it remained as the only tridimensional model of a GPCR, until other receptors were solved [7,8]. The recent structures of the chromophore free protein, opsin, and of the opsin bound to a peptide derived

from the C-terminus of transducin (Gt) unravelled key features regarding the interaction between the receptor and the G-protein, as well as the main changes in TM helices that accompany receptor activation [9,10].

The chromophore, 11-*cis*-retinal, is covalently bound through a protonated Schiff base linkage to K296, residue 7.43 according to the Ballesteros and Weinstein numbering system [11]. The positive charge at the Schiff base is stabilized by the negatively charged counterion E113(3.28). The initial process of rhodopsin activation is a light-induced 11-*cis* to all-*trans* isomerization of the chromophore. Subsequently, the receptor

Abbreviations

adRP, autosomal dominant retinitis pigmentosa; BTP, Bis-Tris-Propane; DM, dodecyl maltoside; GPCR, G-protein coupled receptor; Gt, transducin; Meta, metarhodopsin; RP, retinitis pigmentosa; TM, transmembrane; WT, wild-type.

thermally relaxes on a millisecond timescale to its active conformation proceeding through a number of spectroscopically distinguishable intermediates. A crucial event during this process is the transition from the inactive metarhodopsin I (Meta I), still with a protonated Schiff base, to the active metarhodopsin II (Meta II) state, with a deprotonated Schiff base, which is reflected in a significant shift of the absorption maximum from 480 nm (Meta I) to 380 nm (Meta II). Meta II activates Gt by binding it to its cytoplasmic domain and thereby triggering the visual cascade [12].

Retinitis pigmentosa (RP) belongs to a group of inherited degenerative retinopathies that are genetically and clinically heterogeneous [13,14]. In the past 15 years, more than 150 mutations have been discovered in the opsin gene, most of them associated with an inheritable form of the disease (autosomal dominant retinitis pigmentosa, adRP), involving mainly point mutations and a few deletions. Mutations associated with adRP are spread all over the opsin gene in the three domains of the receptor: intradiscal, TM and cytoplasmic. The study of rhodopsin mutants associated with retinal diseases, such as RP, provides information about the molecular mechanism of these pathologies. The study of GPCRs is also of outstanding pharmacological interest, as this family of receptors is involved in a wide variety of physiological and pathophysiological processes. Therefore, structural and functional studies on rhodopsin provide insights into common structural motifs of GPCRs and allow us to elucidate the structural basis of a proposed common activation mechanism.

TM1 and TM2 play an important role in the stability and function of rhodopsin. The naturally occurring mutations at G51 (1.46), G51A and G51V, and G89D (2.56) of rhodopsin, associated with adRP, were first reported in the early 1990s [15–17]. G51 (1.46) is found in ~50% of class A GPCRs, whereas G89 (2.56) is mostly specific of blue/green vertebrate opsins. G2.56 and G2.57 are present in ~7% of class A GPCRs each and this GG pair is present in 32% of rhodopsins, all belonging to the group of blue/green vertebrate rhodopsins. G89D was tentatively termed class A in a clinical study and was proposed to show an earlier onset and more severity than G51A, which was defined as a class B mutant showing a milder clinical phenotype [18]. The G51V mutant was reported to have normal intracellular trafficking to the plasma membrane similar to wild-type (WT) rhodopsin and little accumulation in the endoplasmic reticulum. This seems to be a common feature of a subset of rhodopsin mutants that may not be classified as folding-defective, like the newly reported G90V adRP mutation [19]. The G51A,

G51V and G89D mutants were studied in the context of the folding and packing of the TM domain together with other adRP mutations in the other TM helices [20]. These studies showed that G51V was able to regenerate with 11-*cis*-retinal to form chromophore-like WT rhodopsin, whereas G51A and G89D could form it only partially [20]. Later, these studies were taken as a starting point for a detailed characterization of the environment of G51 and G89, analysing a series of mutants at these positions [21]. The results provided insights into the structural and functional consequences associated with changes in the size and/or charge of substituted amino acid side-chains at sites of naturally occurring mutations in TM helices I and II [22]. The G51A, G51V and G51L mutant proteins were thermally less stable compared with WT rhodopsin, both in the dark and after photoactivation. Both the stability of the mutants and their ability to activate Gt could be correlated with the increase in size of the side-chain at position 51, pointing to a disruption of the interhelical packing due to the mutations. In the case of mutations at position 89, the charge introduced was found to be more critical than the size of the side-chain. G89 is located next to another glycine, G90 (2.57), whose mutation to aspartic acid is associated with the retinal disease congenital night blindness [23]. Both positions are close to the retinal binding pocket, next to the Schiff base.

There are various important factors that govern rhodopsin activation: *cis-trans* retinal photoisomerization, thermal relaxation of the complex and the pH- and temperature-dependent equilibrium between Meta I and Meta II. At physiological temperature, the equilibrium between Meta I and Meta II conformations is shifted towards Meta II as a result of the rhodopsin–Gt interaction [24]. Upon illumination, the G51V and G89D RP mutants show the formation of a nonactive altered photointermediate that could possibly be in equilibrium with the species described as Meta II.

In the present work, G51V has been combined with mutants E134Q (3.49) and V300G (7.47) to further understand its structural and functional consequences. E134Q is known to shift the Meta I to Meta II equilibrium towards the latter by releasing the neighbouring R135 (3.50) [25], which directly contacts the Gt C-terminus. On the other side, G300 is in intimate contact with G51. The double mutants G51V/E134Q and G51V/V300G helped to determine to which degree the effects of G51V are associated with the D(E)RY or NPxxY micro-switches [26]. Specifically, the additional introduction of E134Q in the background of the G51V mutant structure results in a less altered photointermediate formation and improves Gt activation (0.8 for

the G51V/E134Q double mutant with regard to 0.2 in the G51V single mutant). In this second case, the G51V/V300G mutant still presents an altered photo-intermediate formation and does induce a significant increase in Gt activation, indicating no reversal of the G51V phenotype by V300G. These results reflect that the altered photointermediate formed by G51V and G89D RP mutants could be Meta Ib, described as an inactive species in equilibrium with Meta II and probably with a similar conformation to the active state, but lacking some of the specific structural features that make the receptor functionally active [27]. Overall, our current work, together with previous results, suggests that an alteration in the Meta I to Meta II pathway could be one of the molecular triggers of RP associated with some rhodopsin mutations.

Results

Characterization of G51V and G89D mutants

G51V (1.46) and G89D (2.56) mutants showed an altered photobleaching behaviour, as previously

Table 1. λ_{\max} in the dark and after illumination (light) for WT, G51A, G51V, G89D, G51A/E134Q, G51V/E134Q, V300G and G51V/V300G rhodopsin. Data shown here are the average of several independent purifications.

Rhodopsin	λ_{\max} (dark)	λ_{\max} (light)
WT	500 nm	380 nm
G51A	500 nm	380 nm
G51V	502 nm	380 nm/484 nm
G89D	500 nm	380 nm/490 nm
G51A/E134Q	498 nm	380 nm
G51V/E134Q	501 nm	380 nm/490 nm
V300G	499 nm	380 nm
G51V/V300G	501 nm	380 nm/484 nm

described [15,16]. In contrast to WT protein, G51V and G89D mutants (with λ_{\max} at 502 and 500 nm, in the dark, respectively), were not fully converted to Meta II ($\lambda_{\max} = 380$ nm) after illumination. For the G51V mutant, one band with λ_{\max} at 380 nm and another with λ_{\max} at 484 nm were observed. In the case of the G89D mutant, the species formed after illumination showed two bands with λ_{\max} at 380 and 490 nm (Table 1). These results indicate that G51V and G89D rhodopsin mutants may be trapped in one of the photointermediate states along the activation pathway, and not reaching the active photointermediate, Meta II. The kinetic parameters of formation and disappearance of these altered photointermediates were evaluated. Their stability was determined after 10 s illumination at 20 °C, as measured by the decay of the corresponding absorbance band. For the G51V mutant, the species with λ_{\max} at 484 nm had a decay process with a $t_{1/2}$ of ~ 11 min, whereas for G89D $t_{1/2}$ was ~ 25 min (Table 2). In order to investigate whether these altered photointermediates were in equilibrium with the species formed with λ_{\max} at 380 nm, various experiments were carried out in the presence of 100 μM Gt α -HAA (Gt α -HAA/rhodopsin molar ratio approximately 100 : 1). This is a very high Gt α -HAA/rhodopsin ratio as compared with native photoreceptor cells where the Gt/rhodopsin ratio is much lower, ~ 0.1 . This suggests that *in vivo* the Gt/rhodopsin ratio would not be high enough to shift the mutants' altered photointermediates to their Meta II conformations. The spectra in the dark, after illumination and acidification for G51V and G89D mutants, in the presence of Gt α -HAA (Fig. 1), showed that this altered photointermediate was not formed in the case of the G51V mutant, but it was still formed, although at lower levels, in the case of the G89D mutant. After illumination, the dark species were fully converted to species with λ_{\max} at 380 nm, suggesting that the altered

Table 2. Retinal release, in the presence and in the absence of the Gt α -HAA peptide, Gt activation and $t_{1/2}$ of the altered photointermediate decay process, for WT, G51A, G51V and G89D rhodopsin. The experimental conditions used in the different assays were: (a) 50 mM BTP, pH 7.5, 0.03% DM; (b) 50 mM BTP, pH 7.5, 0.03% DM + 100 μM Gt peptide; (c) 10 mM Tris/HCl, pH 7.1, 100 mM NaCl, 2 mM MgCl₂, 0.012% DM; (d) 10 mM BTP, pH 6.5, 0.03% DM, $T = 20$ °C. Percentage values represent the contribution of each species to the retinal release.

Rhodopsin	(a) Retinal release, $t_{1/2}$ (min)	(b) Retinal release + Gt peptide, $t_{1/2}$ (min)	(c) Maximum ΔF (340 nm) (Gt activation)	(d) Altered photointermediate stability, $t_{1/2}$ (min)
WT	13 \pm 0.1	> 83.0	1.00	–
G51A	18 \pm 0.1	> 83.0	1.0 \pm 0.05	–
G51V	32% 2.0 \pm 0.1 68% 38 \pm 0.5	33.0 \pm 0.4	0.2 \pm 0.02	11.0 \pm 0.1
G89D	19% 2.0 \pm 0.5 81% 23.0 \pm 0.1	38.0 \pm 0.2	0.6 \pm 0.03	25.0 \pm 0.2

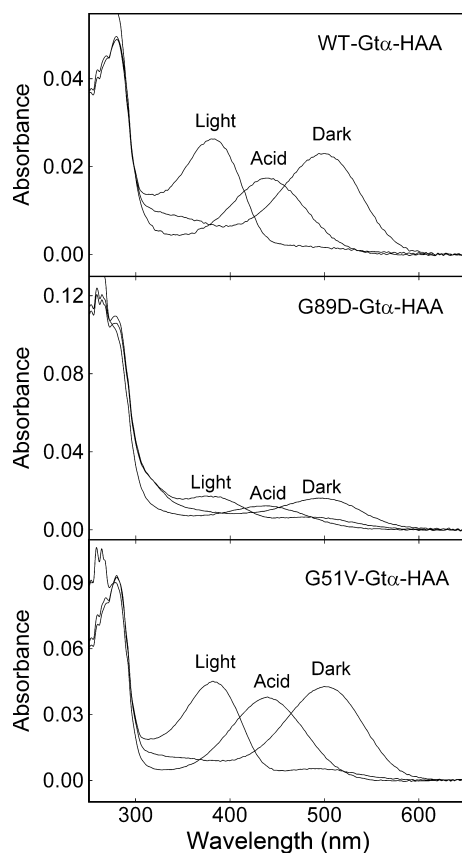


Fig. 1. WT, G51V and G89D UV-visible absorption spectra in the dark, after illumination and after acidification in the presence of 100 μM Gt α -HAA peptide.

species formed in the absence of peptide were all able to reach the Meta II state. The retinal release curve for G51V and G89D mutants at pH 7.5 and 0.03% dodecyl maltoside (DM) could be best fitted to a double-exponential curve, with a slow component and a fast component of retinal release, as described previously [21]. The retinal release in the presence of Gt α -HAA was measured and the results for G51V and G89D were best fitted as single-component exponential rise curves (Table 2). $t_{1/2}$ in the presence of Gt α -HAA for these mutants, compared with $t_{1/2}$ of the WT protein, indicated that both G51V and G89D had a thermally unstable active state. This effect can be correlated with the decrease in Gt activation observed for the mutants. A possible explanation would be that two distinct species in equilibrium are formed after photobleaching: one that is nonfunctional and another one with capacity to activate Gt. Thus, G51V and G89D would also exhibit less stable active photointermediates that would contribute to the reduced degree of Gt activation observed. In terms of the thermal stability, the active

conformation of the G51V mutant was less stable than the active conformation of the mutant G89D and the ability to activate Gt was lower for G51V than for G89D (Table 2). Because of the stronger effect of Gt α -HAA in shifting the altered conformation of G51V, we focused on this mutant for the double mutant studies described in the following sections. The stronger resistance for the altered photointermediate of the G89D mutant to be shifted to the Meta II conformation could be correlated to the more severe phenotype suggested for this mutation [18].

Characterization of G51V double mutants with E134Q and V300G

In order to dissect further the effect of G51V, two double mutants, G51V/E134Q and G51V/V300G, were constructed. The E134Q (3.49) mutation in the conserved D(E)RY motif of class A GPCRs is known to facilitate light-induced Meta II formation [25]. In the present report, E134Q was combined with G51V with the aim of restoring part of the activation lost in the single mutant. A strong relationship between TM1–TM2 and TM7 has been suggested in different reports [21,22,28,29]. Thus, the double mutant G51V/V300G was generated with the purpose of assessing whether or not steric hindrance with V300 (7.47) would be the reason for the large decrease in activation observed for the single G51V, as previously hypothesized [21]. We also constructed mutants G51A/E134Q and V300G as control mutations.

The spectra of the recombinant proteins in the dark, after illumination and acidification, indicated that all the mutants showed normal pigment formation in the dark (Fig. 2). However, G51V/E134Q and G51V/V300G mutants showed an abnormal photobleaching behaviour. Thus, after illumination, UV-visible spectra of the G51V/E134Q mutant showed the formation of two bands, at 380 and 490 nm, respectively. G51V/V300G also showed the formation of an altered intermediate after photobleaching, exhibiting two bands, one at 380 nm and a second one at 483 nm (Table 1). The previous results were obtained with immunopurified rhodopsins in DM solution, but it is usually a concern that the photobleaching behaviour is different in a lipid environment. To clarify the effect of the lipid environment on the photobleaching properties, we prepared COS-1 cell fragments for the WT and G51V/V300G mutant, regenerated them with 11-*cis*-retinal and recorded the dark minus light spectra obtained upon illumination. In spite of the high degree of light scattering of this membrane system, we could detect a difference between the behaviour of the WT

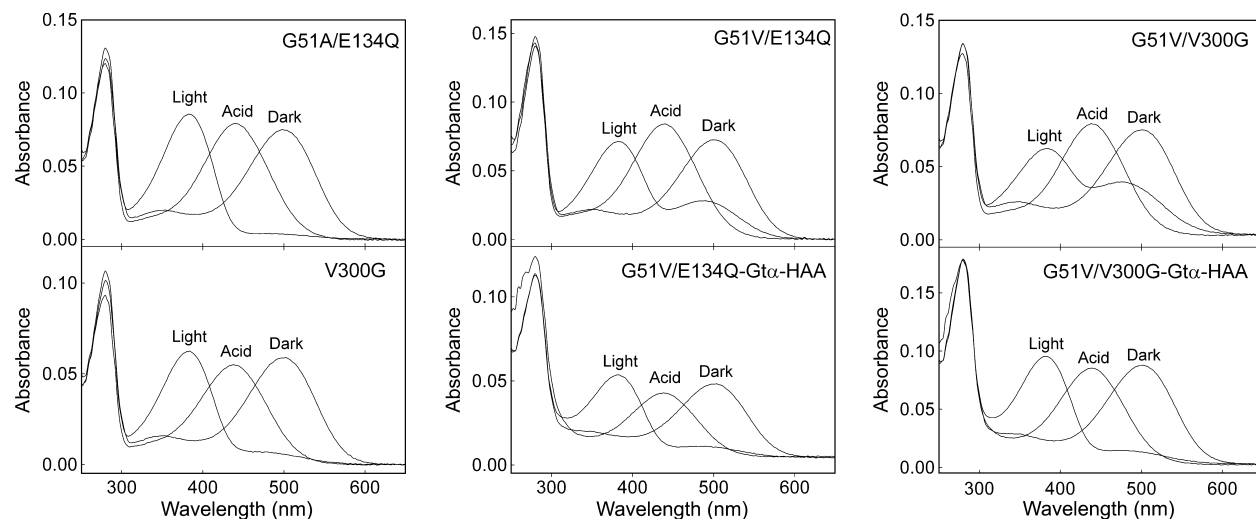


Fig. 2. UV-visible spectra in the dark, after illumination and after acidification in the presence and in the absence of Gt α -HAA, of G51A/E134Q, G51V/E134Q, V300G and G51V/V300G.

and the G51V/V300G double mutant, with the latter showing two bands in the difference spectrum and only one for the WT (data not shown). This difference seems to be consistent with the results obtained in DM solution.

The altered band of these mutants, in DM solution, had less intensity than the corresponding band formed in the case of the G51V single mutant. $t_{1/2}$ for the decay process of the altered photointermediate species of G51V/E134Q and G51V/V300G mutants were determined from the decay of $A_{490\text{ nm}}$ and $A_{484\text{ nm}}$, respectively, at 20 °C. $t_{1/2}$ of the photointermediate formed for the G51V/E134Q mutant was found to be 88 ± 0.3 min, whereas in the case of the G51V/V300G mutant, $t_{1/2}$ was 50 ± 0.3 min. However, G51A/E134Q and V300G mutants showed UV-visible spectra similar to WT, after illumination, with a shift to $A_{380\text{ nm}}$, suggesting that these mutants undergo the same WT photointermediate pathway. In addition, the photobleaching and acidification behaviour of G51V/E134Q and G51V/V300G mutants in the presence of 100 μM Gt α -HAA peptide was analysed. After illumination, both mutants exhibited a single absorption band at 380 nm, and the altered photointermediate band disappeared (Fig. 2). This fact indicates that the altered photointermediates are in equilibrium with the species at 380 nm and that this equilibrium is shifted by the Gt α -HAA peptide towards the species absorbing at 380 nm, presumably the active Meta II conformation.

During the decay of G51V, G51V/E134Q and G51V/V300G mutants we could observe a shift in the

absorption maximum of the characteristic band for the altered photointermediate. The difference spectra between the spectrum recorded at 10 min after illumination and the one recorded immediately after illumination of these mutants showed a shift in the altered photointermediate band from 485–490 nm to 465–470 nm, suggesting the formation of an additional photointermediate (Fig. 3). Interestingly, the existence of equilibria between Meta Ia (485 nm), Meta Ib (465 nm) and Meta II (380 nm) was recently reported [27]. For these mutants, an initial formation of Meta Ia (485 nm), and its decay to Meta Ib (465 nm) before Meta II formation (380 nm), could be observed. Furthermore, in the case of the V300G mutation, the formation of a 470 nm band could be detected shortly after illumination and the progressive disappearance of this band with time could also be observed. This band could correspond to Meta III [30]. In fact, a simple interpretation of the double mutant results would be that the spectral changes observed are due to the conversion of the equilibrium mixture of Meta I, Meta Ib and Meta II to Meta III, which has an absorption maximum at ~ 460 nm. Therefore, the spectral changes observed in the double mutants would indicate the formation of Meta III after establishment of the quasi equilibrium state among Meta I, Meta Ib and Meta II. Experiments at lower temperatures (12 and 4 °C) were carried out to clarify this point. We found a differential behaviour for G51V/V300G and G51V/E134Q, at these lower temperatures, with the latter showing a very slow decay reflected in almost flat difference spectra, but we could not unambiguously determine the contribution of

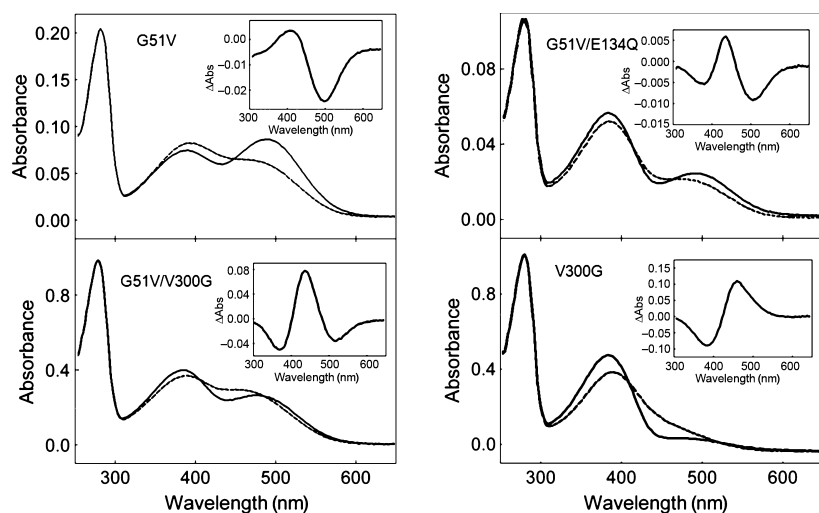


Fig. 3. Absorption spectra of G51V and V300G single mutants and G51V/E134Q and G51V/V300G double mutants, at different times after illumination. Samples were first bleached for 10 s using a 150 W fibreoptic light with a > 495 nm long-pass filter, and spectra were recorded immediately after illumination (—) and 10 min later (---). Difference spectra (10 min minus 0 min) for the illuminated sample spectra are shown in the corresponding insets.

the indicated photointermediates from such experiments (data not shown).

Gt activation

The ability of G51A/E134Q, G51V/E134Q, V300G and G51V/V300G mutants to activate Gt was determined using fluorescence spectroscopy. The fluorescence increase at 340 nm is shown in Fig. 4 for the different mutants, and the maximum value and the initial rates of Gt activation were derived from the fluorescence curves (Table 2). The E134Q single mutant was previously shown to activate Gt at slightly higher levels than WT rhodopsin [31–33]. The G51A/E134Q mutant showed a maximum capacity of activation equal to WT protein, whereas the G51V/E134Q mutant showed a reduced activation of 0.8. V300G and G51V/V300G mutants also showed a decrease in Gt activation with regard to the WT, with maximal activation around 0.6 and 0.2, respectively (Table 3). The initial rates of Gt activation were determined, for each mutant, using the first 100 s from the curve. The G51A/E134Q mutant showed a similar Gt activation rate to the WT protein. Gt activation of the G51V

mutant was reduced below 30% when compared with WT. The introduction of the E134Q mutation, in the G51V mutant sequence background, almost restored the capacity of the protein to activate Gt (0.8 when compared with WT taken as 1.0).

Meta II stability

For each mutant, the Meta II decay was measured by fluorescence increase after illumination of the protein sample. G51V/E134Q, V300G and G51V/V300G mutants showed an exponential curve of retinal release with two components, a slow component and a fast component, like the G51V mutant (Table 2). A correlation could be established between the maximum capacity of Gt activation of these mutants and the stability of their corresponding active states. The mutants showing a higher percentage of unstable component, e.g. fast retinal release component, also showed lower Gt activation levels. Therefore, the G51V/V300G and G51V mutants with a fast component of ~45% and 32%, respectively ($t_{1/2} \sim 2.0$ min), also showed the least Gt activation (0.2) when compared with WT. The unstable component of the G51V/E134Q mutant rep-

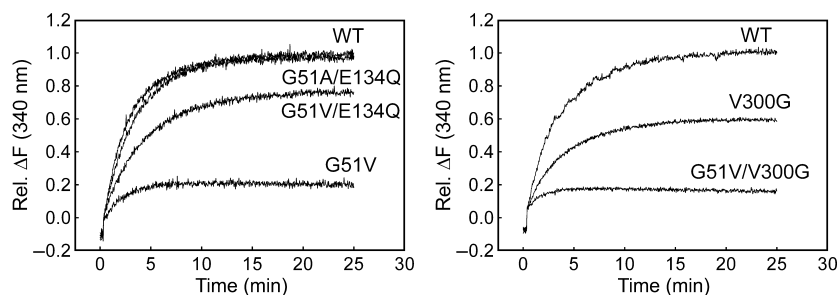


Fig. 4. Gt activation for WT, G51V, G51A/E134Q, G51V/E134Q, V300G and G51V/V300G rhodopsin mutants. The fluorescence increase for all mutants and WT rhodopsins was normalized to WT, taken as 1.00.

Table 3. Initial rates and maximum fluorescence at $\lambda = 340$ nm for Gt activation and $t_{1/2}$ for the retinal release of WT, G51V and V300G single mutants and G51A/E134Q, G51V/E134Q and G51V/V300G double mutants. The fluorescence assay was performed at 20 °C with the following conditions: (a) 50 mM BTP, pH 7.5 containing 0.03% DM; (b,c) 10 mM Tris/HCl, pH 7.1. Initial rates and maximum fluorescence signal for Gt activation are normalized to WT. Data represent the average of at least two independent experiments.

Rhodopsin	(a) Retinal release, $t_{1/2}$ (min)	(b) Maximum ΔF (340 nm) (Gt activation)	(c) Initial rate (Gt activation)
WT	12 ± 0.4	1.00	1.00
G51V	32% 2.0 ± 0.1 68% 38.0 ± 0.5	0.2 ± 0.02	0.3 ± 0.03
G51A/E134Q	–	1.0 ± 0.2	0.8 ± 0.1
G51V/E134Q	20% 8.0 ± 0.3 80% 29.0 ± 0.2	0.8 ± 0.04	0.5 ± 0.02
V300G	45% 2.0 ± 0.2 55% 12.0 ± 0.4	0.6 ± 0.02	0.4 ± 0.02
G51V/V300G	45% 2.0 ± 0.4 55% 12.0 ± 0.4	0.2 ± 0.04	0.2 ± 0.01

resents 20% of the total fluorescence curve with $t_{1/2}$ of 8 min, and Gt activation for this mutant is 0.8 with regard to WT.

Mutational effects in the context of the crystal structures

Figure 5(A,B) displays the location of G/V51 (1.46) in the crystal structures relative to functionally important residues. Position 51 lies just one turn away from the fully conserved N55¹. (1.50) in class A GPCRs. 1GZM crystal structure reveals that the NH of N55 forms two hydrogen bond interactions with the backbones of A299 (7.46) and G51, which stabilize the distorted conformation of TM7 around the NPxxY motif. The same crystal structure contains one water molecule that bridges two additional highly conserved residues: D83 (2.50) (96% of human nonolfactory receptors) and N302 (7.49) (77%) plus the free carbonyl of S298 (7.45). Although not resolved in rhodopsin, two water molecules that have been resolved in the β 2-adrenergic crystal structure are probably conserved through this class of receptor [34]. One of these molecules connects N55 with D83 and also interacts with the water molecule between D83 and N302, thereby providing a link between N55 and N302.

G89 (2.56) is part of the GG motif responsible for the kink of TM2 in the bovine rhodopsin structure, which has been proposed to be conserved [35], and it was proposed that the extracellular portion of TM2

could adopt different conformations depending on the specific features of a receptor [36]. Figure 5D shows how a small change in this segment, by G89D, could change the helix kink and ultimately affect interactions in the vicinity of the retinal (Figure 5D), namely at residues T94 (2.61) and E113 (3.28), decreasing both thermal stability and activation.

Discussion

G51V (1.46) and G89D (2.56) adRP mutants showed an altered photoactivation pathway, forming an abnormal photointermediate that is in equilibrium with Meta II species with λ_{\max} 380 nm. Moreover, the active conformation of these mutants was found to be less thermally stable than the active conformation of WT rhodopsin, a fact that correlated with the changes observed for Gt activation. The G51V mutant, forming a less stable Meta II intermediate than G89D, also showed lower Gt activation (0.20 and 0.57, respectively). Additional mutations E134Q (3.49) and V300G (7.47) were introduced to unravel the nature of the altered photointermediate. On the one side, it has been reported that the E134Q mutation facilitates light-induced Meta II formation [25], as R135 (3.50) has more freedom to adopt the extended conformation that optimally interacts with Gt [9,10]. Figure 5B suggests that E134Q does not require the formation of the hydrogen bond network that connects TM1 to the G-protein for signalling, and thus it becomes almost independent of the structural defects of G51V. Accordingly, the experiments show that E134Q could partially revert the effect of G51V, suggesting that the single mutant G51V would be trapped in an altered photointermediate prior to Meta II formation. On the other side, we added V300G to the G51V mutant to assess whether a valine residue at position 51 could cause steric hindrance with V300 in TM7 [20]. G51V/E134Q and G51V/V300G double mutants formed pigments with dark ground state similar to WT. However, they showed an abnormal photoactivation process, like the G51V single mutant, with the formation of an altered photointermediate, but exhibiting a lower band when compared with G51V. Additionally, in G51V, G51V/E134Q and G51V/V300G, another altered photointermediate ($\lambda_{\max} = 470\text{--}465$ nm) was found prior to Meta II ($\lambda_{\max} = 380$ nm) formation. Recently, the existence of an equilibrium between Meta I species, renamed Meta Ia ($\lambda_{\max} = 485$ nm) and Meta Ib photointermediates ($\lambda_{\max} = 460$ nm), and Meta II ($\lambda_{\max} = 380$ nm) was reported [27]. We propose that our results probably reflect that these mutations influence such equilibrium. Thus, during the

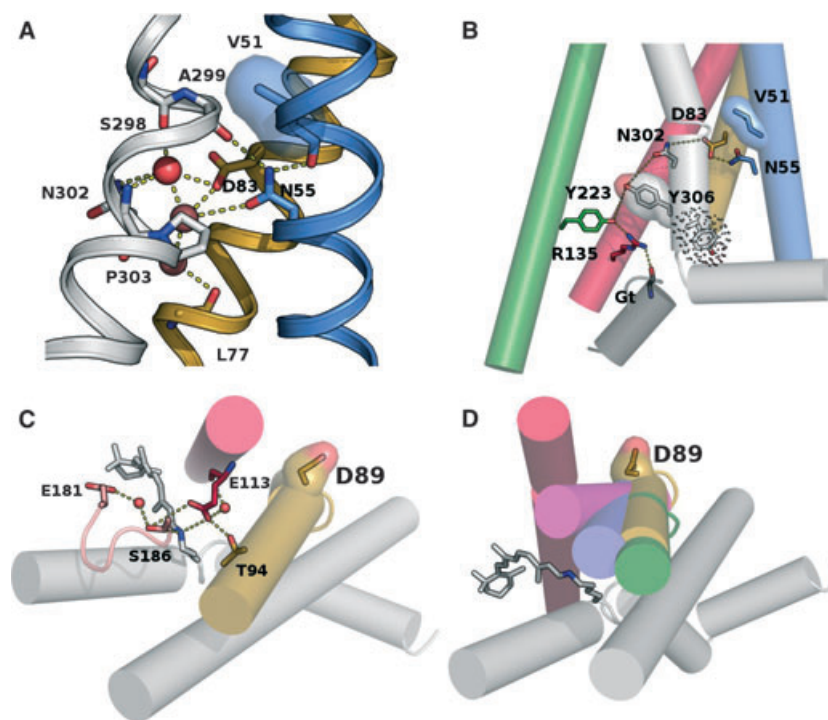


Fig. 5. Mutational effects of G51V and G89D in the context of the crystal structures of dark rhodopsin (A, C and D) and opsin in its Gt binding conformation (B), showing the region around V51 (1.46) (A, B) and around D89 (2.56) and the protonated Schiff base (C, D). Helices are shown as cylinders except in (A), where they are represented with a cartoon; side-chains are sticks coloured by atom-type and crystallographic water molecules are spheres. Hydrogen bond interactions are represented by dashed lines. A van der Waals surface has been added to the mutated residues. Some helices have been omitted for better clarity. (A) The network of hydrogen bond interactions that involve the conserved N55 (1.50) and the backbone of G51. The colour code for the TM helices is TM1 (blue), TM2 (yellow) and TM7 (white). Brown spheres correspond to water molecules taken from 2RH1, whereas those present in 1GZM are displayed in red. (B) The proximity of V51 to the network of polar residues connecting TM1 (blue), TM2 (yellow), TM3 (red), TM5 (green) and TM7 + helix 8 (white) with the Gt C-terminus (grey). A van der Waals surface has been added to Y306 to outline the different conformation compared with the inactive state (represented with a dotted surface). (C) Polar residues and crystallographic water molecules that participate in association with the protonated Schiff base. The colour code of the helices is: TM2 (gold), TM3 (red), TM1 and TM7 + short helix 8 (white). (D) Different conformations of the extracellular part of TM2 in various crystal structures: *Tadarodes pacificus* rhodopsin [pdb:1GZM, 56] (green), β_2 adrenergic [pdb:2RH1, 57] (blue) and adenosine A₂ [pdb:3EML, 60] (magenta).

photoactivation process of these mutants, we would be observing the initial formation of the Meta Ia photointermediate and its decay to the Meta Ib before Meta II formation.

Meta II stability for these mutants was measured by retinal release, and the functionality of the process was determined by means of Gt activation assays. All mutants showed a double-exponential curve for retinal release with a fast and a slow component. The Gt activation and the fast retinal release component correlated well for these mutants: more unstable mutants with a fast retinal release also showed lower Gt activation rates. Therefore, G51V/V300G and G51V, in which the fast component contributes 45 and 32%, respectively, to retinal release, produced the lowest Gt activation (0.2 when compared with WT). The unstable

component of the G51V/E134Q mutant represents ~20% of the total protein with $t_{1/2} = 8$ min, and its maximum Gt activation is ~0.8 with regard to WT rhodopsin. E134Q mutation partially reverted to the G51V phenotype, partially recovering the receptor functionality. By contrast, introduction of the V300G mutation in the G51V mutant structure did not improve receptor functionality. Both mutants involving V300G showed a reduction in the ability to activate Gt. The specific initial rates of activation were 0.4 for G51V/V300G and 0.2 for V300G. This suggests that alterations associated with N55 (1.50) would be more important than the possible steric clashes between TM1 and TM7. Thus, the introduction of the V300G mutation in G51V protein did not increase the activation of the single mutant. Indeed, molecular

models reveal that the V300G mutant can be tolerated both in the inactive and in the G-protein binding states.

In view of all this experimental evidence, we propose that the mutants in the present study follow an activation pathway that includes the initial formation of a Meta I photointermediate, renamed Meta Ia, and the decay to Meta Ib [27]. The Meta Ib photointermediate would display structural differences compared with the Meta Ia state that could probably make it more similar to Meta II, but without its functional capacity [27]. G51V affects packing between TM1, TM2 and TM7 and modulates the interactions between important amino acids in the Meta I to Meta II equilibrium [37,38]. D83 (2.50) has an important role in Meta II formation; mutations in this amino acid affect such an equilibrium and the D83 environment changes during the photoactivation process [37,39]. This amino acid interacts with the NPxxY motif, in helix 7, through a cluster of water molecules and forms a hydrogen bond with the neighbouring N55 (1.50) [39–41]. The crystal structure of opsin bound to Gt shown in Fig. 5B reveals that a large movement of the 91% conserved Y306 (7.53) extends this network of hydrogen bond interactions, providing a direct link between N55 and the G-protein C-terminus (Fig. 5A). The cartoons illustrate how the increasing side-chain volumes at G51 would necessarily lead to distortions at the preceding network associated with the NPxxY motif, a fact that would be compatible with the experimental features of the G51V mutant. Reduced G-protein activation, due to mutation of D83 (2.50) pivot to asparagine or alanine, is known for a large number of opsin-like nonvisual receptors. The creation of a second switch by a change at G89 (2.56), from glycine to aspartic acid, may point to a difference in bundling of TM helices in visual and non-visual A-GPCRs, perhaps due to the lack of the opsin-obligatory interaction K296 (7.43) in the latter.

In the context of the crystal structures (Fig. 5), the G51V mutation changes the environment of D83, thereby modifying the interactions involved in the Meta I to Meta II equilibrium by shifting it towards an inactive photointermediate, which could alter photoreceptor cell proteostasis. Thus, the lack of signalling may not be the triggering cause of photoreceptor cell death, but light-induced accumulation of the analysed photointermediate. If that hypothesis is correct, dark rearing of mice carrying these mutations could rescue rods from degeneration. Further studies with transgenic animals would be needed to confirm this.

A recent study on the pharmacological rescue of rhodopsin RP mutants has proposed that abnormal photoactivity, characterized by Meta I-like photopro-

ducts, would contribute to the phenotype [42]. Another recent study detected four metastable states in the transition between inactive and opsin-like structures, with at least two activated conformations characterized by a different extent of separation between TM3 and TM6 [43]. Although protein misfolding has been proposed as the molecular cause of RP for many rhodopsin mutations [42], other mechanisms have also been suggested [44]. Spectroscopic studies classify rhodopsin mutations as misfolding mutations on the basis of an altered A_{280}/A_{500} ratio in the absorbance spectra [20]. This would mean that the misfolded protein is unable to correctly bind the 11-*cis*-retinal chromophore. However, it is well known that rhodopsin is more stable when inserted into the membrane than in a detergent-solubilized state [45]. Mutant analysis requires purification in detergent, which can cause instability of the chromophore, resulting in higher A_{280}/A_{500} ratios, which may not necessarily reflect misfolding of the protein. Furthermore, many studies claiming that mutations in rhodopsin cause RP mainly by protein misfolding are based on the detailed characterization of a subset of mutants and no subcellular localization has been reported for many of these mutations [44]. In our case, the nonfunctional Meta I-like photointermediates here observed would form upon rhodopsin photobleaching and would abnormally accumulate, causing toxic effects on photoreceptor cells, leading to their degeneration. Our study unravels the nature of these photointermediates in *in vitro*-purified mutants and adds on the complexity of molecular mechanisms, other than protein misfolding, associated with RP retinal degeneration.

Materials and methods

Materials

11-*cis*-retinal was a gift from Professor A. R. de Lera (Universidad de Vigo, Spain) and Rosalie Crouch (University of South Carolina and the National Eye Institute, National Institutes of Health, USA). Purified mAb rho-1D4 was obtained from the National Culture Center (Minneapolis, MN, USA) and was coupled to CNBr-activated Sepharose 4 Fast Flow (Amersham Pharmacia Biotech, Piscataway, NJ, USA). DM (*n*-dodecyl- β -D-maltoside; dodecyl maltoside) was purchased from Biomol (Hamburg, Germany). COS-1 cells (ATCC no. CRL-1650) were obtained from American Type Culture Collection (Manassas, VA, USA). CompleteTM protease inhibitor mixture was obtained from Roche Molecular Biochemicals (Mannheim, Germany) and was used at a concentration of one tablet in 75 mL buffer.

Construction of opsin mutants

Mutations were introduced into the synthetic bovine opsin gene [46] by replacement of a *BclI-HindIII* restriction fragment by synthetic DNA duplexes containing the required codon changes in the case of the mutants at position 51. For the mutants at position 89, the restriction fragment replaced was *BglII-NcoI*. The mutant genes were cloned in the pMT4 vector [47] as described previously [20,48,49]. Mutations at position 89 were carried out using a pSK vector [50] derived from the vector pCMV5 [51]. V300G mutations were introduced by site-directed mutagenesis on WT and G51V sequences. G51A/E134Q and G51V/E134Q were constructed by cassette mutagenesis from the initial mutations G51A, G51V and E134Q. The correct sequence of mutations introduced was confirmed by the dideoxy chain-terminated method.

Expression and purification of WT and rhodopsin mutants

WT and mutant opsin genes were expressed in transiently transfected monkey kidney cells (COS-1) as described previously [33]. After the addition of 30 μM 11-*cis*-retinal in the dark, the transfected COS-1 cells were solubilized in 1% DM, and the proteins were purified by immunoaffinity chromatography. Rhodopsin was eluted in 10 mM Bis-Tris-Propane (BTP) pH 6.5, 0.03% DM and the correctly folded fractions [48] of these mutants were the ones used in the present study.

UV-visible absorption spectra of WT and rhodopsin mutants

Spectra were acquired at 20 °C with a Varian Cary 50 UV-visible spectrometer or with a Varian Cary 100Bio spectrophotometer equipped with water-jacketed cuvette holders connected to a circulating water bath. All spectra were recorded with a bandwidth of 2 nm. For photobleaching experiments, samples were illuminated with a 150 W fibre-optic light equipped with a > 495 nm long-pass filter for 10 s, and the corresponding bleached spectrum was recorded immediately after illumination. Acidification of the samples was carried out with 10 μL HCl 1M (1/10 dilution). Preliminary tests at different pHs, ranging between 5 and 8, revealed that the formation of the altered photo-intermediate species is not dramatically influenced by pH.

Rate of Meta II decay as measured by retinal release

The rate of retinal release, which parallels the Meta II decay of the protein in the case of the WT under the conditions used, was studied using fluorescence spectroscopy,

essentially as described previously [52]. Typically, 2.4 μg of pigment in a volume of 120 μL 200 mM BTP pH 7.5 and 0.03% DM was used. For the assay, the excitation and emission wavelengths were 295 nm (slit, 0.2 nm) and 330 nm (slit, 4 nm), respectively. The samples were bleached for 10 s, and the fluorescence increase was measured. The assay was also performed in parallel using the same conditions except that the retinal release was measured in the presence of 100 μM Gt α -HAA, a high-affinity peptide consisting of residues 340–350 of the Gt α -subunit C-terminal domain. This peptide, with sequence VLEDLKSCGLF, is known to efficiently stabilize the active Meta II state [53,54]. Spectra obtained were normalized and fitted to single- or double-exponential functions using SIGMAPLOT (Jandel Scientific, Chicago, IL, USA).

Gt activation assay

Gt was purified from bovine retina and stored in 20 mM BTP, pH 7.1, 130 mM NaCl, 1 mM MgCl₂, 1 mM dithiothreitol. Fluorescence measurements were performed using a Fluorolog 2 (Spex Industries, Metuchen, NJ, USA) fluorescence spectrophotometer, as previously described [55]. Briefly, 2 nM pigment and 250 nM Gt in 20 mM BTP (pH 7.5), 130 mM NaCl, 1 mM MgCl₂, containing 0.01% DM and 5 μM guanosine 5-[γ]-thio triphosphate in a final volume of 650 μL ; spectra were normalized to the fluorescence intensity of the sample before illumination. For determining the rates of Gt activation, the initial slopes of the first 30–60 s of data after illumination were fitted by linear regression.

Molecular modelling

Models of inactive rhodopsin mutants were constructed on the basis of the crystal structure PDB:1GZM [56], whereas the active models relied on the opsin structure crystallized with a peptide based on Gt C-terminus:3DQB [10]. All crystallographic water molecules were kept and additional ones, present in β 2 adrenergic structures 2RH1 [57] that are probably present in rhodopsin and other class A GPCRs, were incorporated into the working models. The conformations of the mutated side-chains were selected based on a library of rotamers implemented in PYMOL [58]. All systems were energy minimized in bulk using the AMBER99SB force field [59]. All figures were created using PYMOL [58].

Acknowledgements

We thank E. Ritter, F. Bartl and O. P. Ernst for helpful discussions, and C. Koch, R. Hauer, H. Seibel and K. Engel for excellent technical assistance. This research was supported by grants from Ministerio de Investigación, Ciencia e Innovación (SAF2005-08148-C04-02 and SAF2008-04943-C02-02 to PG), UPC

fellowship (fellowship from Universitat Politècnica de Catalunya to LB-P), fellowship from Generalitat de Catalunya (BE-2004 to LB-P), and contract grant from the Instituto de Salud Carlos III to AC.

References

- Hargrave PA (2001) Rhodopsin structure, function, and topography the Friedenwald lecture. *Invest Ophthalmol Vis Sci* **42**, 3–9.
- Sakmar TP, Menon ST, Marin EP & Awad ES (2002) Rhodopsin: insights from recent structural studies. *Annu Rev Biophys Biomol Struct* **31**, 443–484.
- Bockaert J & Pin JP (1999) Molecular tinkering of G protein-coupled receptors: an evolutionary success. *EMBO J* **18**, 1723–1729.
- Wess J (1997) G-protein-coupled receptors: molecular mechanisms involved in receptor activation and selectivity of G-protein recognition. *FASEB J* **11**, 346–354.
- Marinissen MJ & Gutkind JS (2001) G-protein-coupled receptors and signaling networks: emerging paradigms. *Trends Pharmacol Sci* **22**, 368–376.
- Palczewski K, Kumasaka T, Hori T, Behnke CA, Motoshima H, Fox BA, Le Trong I, Teller DC, Okada T, Stenkamp RE *et al.* (2000) Crystal structure of rhodopsin: a G protein-coupled receptor. *Science* **289**, 739–745.
- Rasmussen SG, Choi HJ, Rosenbaum DM, Kobilka TS, Thian FS, Edwards PC, Burghammer M, Ratnala VR, Sanishvili R, Fischetti RF *et al.* (2007) Crystal structure of the human beta2 adrenergic G-protein-coupled receptor. *Nature* **450**, 383–387.
- Warne T, Serrano-Vega MJ, Baker JG, Moukhametzianov R, Edwards PC, Henderson R, Leslie AG, Tate CG & Schertler GF (2008) Structure of a beta1-adrenergic G-protein-coupled receptor. *Nature* **454**, 486–491.
- Park JH, Scheerer P, Hofmann KP, Choe HW & Ernst OP (2008) Crystal structure of the ligand-free G-protein-coupled receptor opsin. *Nature* **454**, 183–187.
- Scheerer P, Park JH, Hildebrand PW, Kim YJ, Krauss N, Choe HW, Hofmann KP & Ernst OP (2008) Crystal structure of opsin in its G-protein-interacting conformation. *Nature* **455**, 497–502.
- Ballesteros JA & Weinstein H (1995) Integrated methods for the construction of three-dimensional models and computational probing of structure–function relations in G protein-coupled receptors. *Methods Neurosci* **25**, 366–428.
- Scheerer P, Heck M, Goede A, Park JH, Choe HW, Ernst OP, Hofmann KP & Hildebrand PW (2009) Structural and kinetic modeling of an activating helix switch in the rhodopsin–transducin interface. *Proc Natl Acad Sci USA* **106**, 10660–10665.
- Berson EL (1993) Retinitis pigmentosa. The Friedenwald Lecture. *Invest Ophthalmol Vis Sci* **34**, 1659–1676.
- Farrar GJ, Kenna PF & Humphries P (2002) On the genetics of retinitis pigmentosa and on mutation-independent approaches to therapeutic intervention. *EMBO J* **21**, 857–864.
- Dryja TP, Hahn LB, Cowley GS, McGee TL & Berson EL (1991) Mutation spectrum of the rhodopsin gene among patients with autosomal dominant retinitis pigmentosa. *Proc Natl Acad Sci USA* **88**, 9370–9374.
- Sung CH, Davenport CM, Hennessey JC, Maumenee IH, Jacobson SG, Heckenlively JR, Nowakowski R, Fishman G, Gouras P & Nathans J (1991) Rhodopsin mutations in autosomal dominant retinitis pigmentosa. *Proc Natl Acad Sci USA* **88**, 6481–6485.
- Macke JP, Davenport CM, Jacobson SG, Hennessey JC, Gonzalez-Fernandez F, Conway BP, Heckenlively J, Palmer R, Maumenee IH, Sieving P *et al.* (1993) Identification of novel rhodopsin mutations responsible for retinitis pigmentosa: implications for the structure and function of rhodopsin. *Am J Hum Genet* **53**, 80–89.
- Cideciyan AV, Hood DC, Huang Y, Banin E, Li ZY, Stone EM, Milam AH & Jacobson SG (1998) Disease sequence from mutant rhodopsin allele to rod and cone photoreceptor degeneration in man. *Proc Natl Acad Sci USA* **95**, 7103–7108.
- Neidhardt J, Barthelmes D, Farahmand F, Fleischhauer JC & Berger W (2006) Different amino acid substitutions at the same position in rhodopsin lead to distinct phenotypes. *Invest Ophthalmol Vis Sci* **47**, 1630–1635.
- Hwa J, Garriga P, Liu X & Khorana HG (1997) Structure and function in rhodopsin: packing of the helices in the transmembrane domain and folding to a tertiary structure in the intradiscal domain are coupled. *Proc Natl Acad Sci USA* **94**, 10571–10576.
- Bosch L, Ramon E, Del Valle LJ & Garriga P (2003) Structural and functional role of helices I and II in rhodopsin. A novel interplay evidenced by mutations at Gly-51 and Gly-89 in the transmembrane domain. *J Biol Chem* **278**, 20203–20209.
- Abdulaev NG (2003) Building a stage for interhelical play in rhodopsin. *Trends Biochem Sci* **28**, 399–402.
- Rao VR, Cohen GB & Oprian DD (1994) Rhodopsin mutation G90D and a molecular mechanism for congenital night blindness. *Nature* **367**, 639–642.
- Okada T, Ernst OP, Palczewski K & Hofmann KP (2001) Activation of rhodopsin: new insights from structural and biochemical studies. *Trends Biochem Sci* **26**, 318–324.
- Herrmann R, Heck M, Henklein P, Kleuss C, Hofmann KP & Ernst OP (2004) Sequence of interactions in receptor–G protein coupling. *J Biol Chem* **279**, 24283–24290.

- 26 Nygaard R, Frimurer TM, Holst B, Rosenkilde MM & Schwartz TW (2009) Ligand binding and micro-switches in 7TM receptor structures. *Trends Pharmacol Sci* **30**, 249–259.
- 27 Shichida Y & Morizumi T (2007) Mechanism of G-protein activation by rhodopsin. *Photochem Photobiol* **83**, 70–75.
- 28 Xu W, Campillo M, Pardo L, Kim de Riel J & Liu-Chen LY (2005) The seventh transmembrane domains of the delta and kappa opioid receptors have different accessibility patterns and interhelical interactions. *Biochemistry* **44**, 16014–16025.
- 29 Bee MS & Hulme EC (2007) Functional analysis of transmembrane domain 2 of the M1 muscarinic acetylcholine receptor. *J Biol Chem* **282**, 32471–32479.
- 30 Heck M, Schadel SA, Mareztki D, Bartl FJ, Ritter E, Palczewski K & Hofmann KP (2003) Signaling states of rhodopsin. Formation of the storage form, metarhodopsin III, from active metarhodopsin II. *J Biol Chem* **278**, 3162–3169.
- 31 Acharya S, Saad Y & Karnik SS (1997) Transducin-alpha C-terminal peptide binding site consists of C-D and E-F loops of rhodopsin. *J Biol Chem* **272**, 6519–6524.
- 32 Sakmar TP, Franke RR & Khorana HG (1989) Glutamic acid-113 serves as the retinylidene Schiff base counterion in bovine rhodopsin. *Proc Natl Acad Sci USA* **86**, 8309–8313.
- 33 Ramon E, Cordomi A, Bosch L, Zernii EY, Senin II, Manyosa J, Philippov PP, Perez JJ & Garriga P (2007) Critical role of electrostatic interactions of amino acids at the cytoplasmic region of helices 3 and 6 in rhodopsin conformational properties and activation. *J Biol Chem* **282**, 14272–14282.
- 34 Nygaard R, Valentin-Hansen L, Mokrosinski J, Frimurer TM & Schwartz TW (2010) Conserved water-mediated hydrogen bond network between TM-I, -II, -VI, and -VII in 7TM receptor activation. *J Biol Chem* **285**, 19625–19636.
- 35 Ballesteros JA, Shi L & Javitch JA (2001) Structural mimicry in G protein-coupled receptors: implications of the high-resolution structure of rhodopsin for structure–function analysis of rhodopsin-like receptors. *Mol Pharmacol* **60**, 1–19.
- 36 Deupi X, Dolker N, Lopez-Rodriguez ML, Campillo M, Ballesteros JA & Pardo L (2007) Structural models of class A G protein-coupled receptors as a tool for drug design: insights on transmembrane bundle plasticity. *Curr Top Med Chem* **7**, 991–998.
- 37 Breikers G, Bovee-Geurts PH, DeCaluwe GL & DeGrip WJ (2001) A structural role for Asp83 in the photoactivation of rhodopsin. *Biol Chem* **382**, 1263–1270.
- 38 Okada T, Fujiyoshi Y, Silow M, Navarro J, Landau EM & Shichida Y (2002) Functional role of internal water molecules in rhodopsin revealed by X-ray crystallography. *Proc Natl Acad Sci USA* **99**, 5982–5987.
- 39 Lehmann N, Alexiev U & Fahmy K (2007) Linkage between the intramembrane H-bond network around aspartic acid 83 and the cytosolic environment of helix 8 in photoactivated rhodopsin. *J Mol Biol* **366**, 1129–1141.
- 40 Urizar E, Claeysen S, Deupi X, Govaerts C, Costagliola S, Vassart G & Pardo L (2005) An activation switch in the rhodopsin family of G protein-coupled receptors: the thyrotropin receptor. *J Biol Chem* **280**, 17135–17141.
- 41 Pardo L, Deupi X, Dolker N, Lopez-Rodriguez ML & Campillo M (2007) The role of internal water molecules in the structure and function of the rhodopsin family of G protein-coupled receptors. *Chembiochem* **8**, 19–24.
- 42 Krebs MP, Holden DC, Joshi P, Clark CL III, Lee AH & Kaushal S (2010) Molecular mechanisms of rhodopsin retinitis pigmentosa and the efficacy of pharmacological rescue. *J Mol Biol* **395**, 1063–1078.
- 43 Provasi D & Filizola M (2010) Putative active states of a prototypic g-protein-coupled receptor from biased molecular dynamics. *Biophys J* **98**, 2347–2355.
- 44 Mendes HF, van der Spuy J, Chapple JP & Cheetham ME (2005) Mechanisms of cell death in rhodopsin retinitis pigmentosa: implications for therapy. *Trends Mol Med* **11**, 177–185.
- 45 del Valle LJ, Ramon E, Canavate X, Dias P & Garriga P (2003) Zinc-induced decrease of the thermal stability and regeneration of rhodopsin. *J Biol Chem* **278**, 4719–4724.
- 46 Ferretti L, Karnik SS, Khorana HG, Nassal M & Oprian DD (1986) Total synthesis of a gene for bovine rhodopsin. *Proc Natl Acad Sci USA* **83**, 599–603.
- 47 Franke RR, Sakmar TP, Oprian DD & Khorana HG (1988) A single amino acid substitution in rhodopsin (lysine 248–leucine) prevents activation of transducin. *J Biol Chem* **263**, 2119–2122.
- 48 Liu X, Garriga P & Khorana HG (1996) Structure and function in rhodopsin: correct folding and misfolding in two point mutants in the intradiscal domain of rhodopsin identified in retinitis pigmentosa. *Proc Natl Acad Sci USA* **93**, 4554–4559.
- 49 Garriga P, Liu X & Khorana HG (1996) Structure and function in rhodopsin: correct folding and misfolding in point mutants at and in proximity to the site of the retinitis pigmentosa mutation Leu-125-> Arg in the transmembrane helix C. *Proc Natl Acad Sci USA* **93**, 4560–4564.
- 50 Kaushal S & Khorana HG (1994) Structure and function in rhodopsin. 7. Point mutations associated with autosomal dominant retinitis pigmentosa. *Biochemistry* **33**, 6121–6128.
- 51 Andersson S, Davis DL, Dahlback H, Jornvall H & Russell DW (1989) Cloning, structure, and expression

- of the mitochondrial cytochrome P-450 sterol 26-hydroxylase, a bile acid biosynthetic enzyme. *J Biol Chem* **264**, 8222–8229.
- 52 Farrens DL & Khorana HG (1995) Structure and function in rhodopsin. Measurement of the rate of metarhodopsin II decay by fluorescence spectroscopy. *J Biol Chem* **270**, 5073–5076.
- 53 Bartl F, Ritter E & Hofmann KP (2000) FTIR spectroscopy of complexes formed between metarhodopsin II and C-terminal peptides from the G-protein alpha- and gamma-subunits. *FEBS Lett* **473**, 259–264.
- 54 Martin EL, Rens-Domiano S, Schatz PJ & Hamm HE (1996) Potent peptide analogues of a G protein receptor-binding region obtained with a combinatorial library. *J Biol Chem* **271**, 361–366.
- 55 Fritze O, Filipek S, Kuksa V, Palczewski K, Hofmann KP & Ernst OP (2003) Role of the conserved NPxxY(x)5,6F motif in the rhodopsin ground state and during activation. *Proc Natl Acad Sci USA* **100**, 2290–2295.
- 56 Li J, Edwards PC, Burghammer M, Villa C & Schertler GF (2004) Structure of bovine rhodopsin in a trigonal crystal form. *J Mol Biol* **343**, 1409–1438.
- 57 Cherezov V, Rosenbaum DM, Hanson MA, Rasmussen SG, Thian FS, Kobilka TS, Choi HJ, Kuhn P, Weis WI, Kobilka BK *et al.* (2007) High-resolution crystal structure of an engineered human beta2-adrenergic G protein-coupled receptor. *Science* **318**, 1258–1265.
- 58 The PyMOL Molecular Graphics Systems, Version 1.2b5. DeLano Scientific.
- 59 Hornak V, Abel R, Okur A, Strockbine B, Roitberg A & Simmerling C (2006) Comparison of multiple Amber force fields and development of improved protein backbone parameters. *Proteins* **65**, 712–725.
- 60 Jaakola VP, Griffith MT, Hanson MA, Cherezov V, Chien YET, Lane JR, Ijzerman AP & Stevens RC (2008) The 2.6 angstrom crystal structure of a human 2A2 adenosine receptor bound to an antagonist. *Science* **322**, 1211–1217.